Discovery of Highly Selective and Potent p38 Inhibitors Based on a Phthalazine Scaffold[#]

Brad Herberich,*[,†] Guo-Qiang Cao,[†] Partha P. Chakrabarti,[†] James R. Falsey,[†] Liping Pettus,[†] Robert M. Rzasa,[†] Anthony B. Reed,[†] Andreas Reichelt,[†] Kelvin Sham,[†] Maya Thaman,[†] Ryan P. Wurz,[†] Shimin Xu,[†] Dawei Zhang,[†] Faye Hsieh,[‡] Matthew R. Lee,[§] Rashid Syed,[§] Vivian Li,[§] David Grosfeld,[§] Matthew H. Plant,[⊥] Bradley Henkle,[⊥] Lisa Sherman,[⊥] Scot Middleton,[⊥] Lu Min Wong,[⊥] and Andrew S. Tasker[†]

Departments of Medicinal Chemistry, Inflammation, Pharmacokinetics and Drug Metabolism, and Molecular Structure, Amgen, Inc., One Amgen Center Drive, Thousand Oaks, California 91320-1799

Received May 9, 2008

Investigations into the structure−activity relationships (SAR) of a series of phthalazine-based inhibitors of p38 are described. These efforts originated from quinazoline **1** and through rational design led to the development of a series of orally bioavailable, potent, and selective inhibitors. Kinase selectivity was achieved by exploiting a collection of interactions with p38α including close contact to Ala157, occupation of the hydrophobic gatekeeper pocket, and a residue flip with Gly110. Substitutions on the phthalazine influenced the pharmacokinetic properties, of which compound **16** displayed the most desirable profile. Oral dosing (0.03 mg/kg) of **16** in rats 1 h prior to LPS challenge gave a >50% decrease in TNFα production.

Introduction

The excess production of the inflammatory cytokine tumor necrosis factor-α (TNFα[a]) is associated with a number of inflammatory diseases including rheumatoid arthritis and psoriasis.[1] There are a number of anti-TNFα therapies that bind and inhibit TNFα including etanercept (a soluble TNFα receptor−immunoglobulin fusion protein), adalimumab (a fully human monoclonal antibody), and infliximab (a mouse−human chimeric TNFα antibody) for the treatment of inflammatory diseases.[1,2] Although these injectable biological drugs have made a dramatic impact on patients' lives, they have associated side effects.[3] The next generation of anti-inflammatory agents could be orally available agents that decrease the production of TNFα. The mitogen activated protein kinase (MAPK) p38 has been shown to be a major signaling molecule in the production of inflammatory cytokines, and its therapeutic potential has been reviewed.[4] Of the four isoforms, p38α appears to be the dominant player.[5] For more than a decade, extensive efforts have been made to develop an orally available p38α inhibitor for the treatment of inflammatory diseases,[6] and in this report we outline our progress toward this goal.

The initial quinazoline lead (**1**, Figure 1) demonstrated nanomolar activity against p38α but suffered a lack of selectivity against other kinases. An X-ray crystal structure of **1** bound to p38α gave insights into a rational redesign to improve selectivity (Figure 2). Quinazoline **1** binds to p38α, forming a classical donor−acceptor pair interaction with Met109 on the linker strand; the methyl group on the toluamide ring occupies the hydrophobic "gatekeeper" pocket lined with Thr106, Val105,

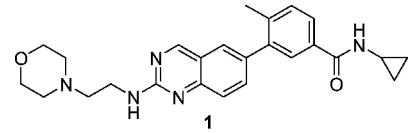

1

	IC_{50} (nM)
p38α	2.4±1.3
Kdr	10.5*
Lck	122±20
cKit	162*
JNK1	>10,000*
JNK2	629*
JNK3	788*

Figure 1. Activity of quinazoline **1**. Standard deviation is given when $n > 2$. The asterisk (*) designates an average of two values.

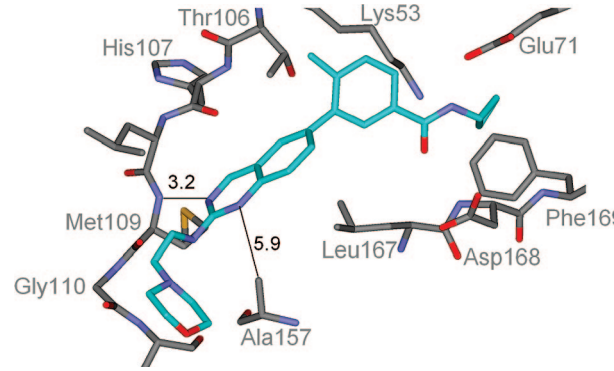

Figure 2. Cocrystal of quinazoline **1** and p38α.

and Leu104. The inhibitor accepts a hydrogen bond from the backbone N−H of Asp168 located on the activation loop and donates a hydrogen bond to the carboxylate side chain of Glu71 located on helix C. The morpholine side chain is solvent exposed and does not significantly contribute to binding. As such, compound **1** engages generic kinase architecture shared by the

[#] Atomic coordinates and structure factors for cocrystal structures of compounds **1** and **19** with p38α can be accessed using PDB codes 3DT1 and 3DS6, respectively.

* To whom correspondence should be addressed. Phone: 805-447-9963. Fax: 805-480-4532. E-mail: brad.herberich@amgen.com.

[†] Department of Medicinal Chemistry.

[‡] Department of Pharmacokinetics and Drug Metabolism.

[§] Department of Molecular Structure.

[⊥] Department of Inflammation.

[a] Abbreviations: TNFα, tumor necrosis factor α; MAPK, mitogen activated protein kinase; PDGF, platelet-derived growth factor; JNK, c-Jun N-terminal kinase; LPS, lipopolysaccharide; CL, clearance; *F*, bioavailability; IL-8, interleukin 8.

10.1021/jm8005417 CCC: $40.75
Published on Web 09/26/2008

Scheme 1. Synthesis of 1-Aminophthalazines **7**−**10**[a]

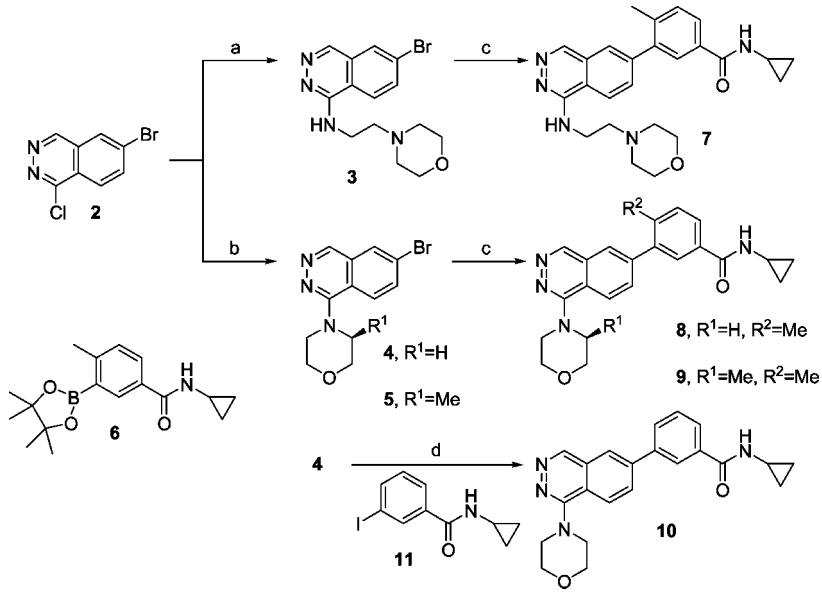

[a] Reagents: (a) 4-(2-aminoethyl)morpholine, *i*-PrOH, 180 °C; (b) morpholine, K_2CO_3, CH_3CN, 160 °C or (*S*)-3-methyl morpholine, Cs_2CO_3, CH_3CN, 200 °C; (c) **6**, $Pd(PPh_3)_4$, 2 M aqueous K_2CO_3, DME/EtOH, 90 °C; (d) (i) bis(pinacolato)diboron, $Pd(dppf)Cl_2$, KOAc, dioxane, 80 °C, (ii) **11**, $Pd(PPh_3)_4$, 1.5 M aqueous K_2CO_3, EtOH, 80 °C.

PDGF and Src family kinases, and this explains a lack of selectivity against these proteins. Comparison of the ATP-binding sites of p38α, Src and PDGF family kinases reveals a number of residue differences. In PDGF, ATP forms a bidentate interaction with the "hinge" or "linker stand" located between the N- and C-terminal lobes of the kinase. It is supported from below by Leu393 located on a β-sheet behind the linker strand. This leucine is present in the vast majority of kinases with a few exceptions; for example, this residue is methionine in cMet, Akt, and insulin receptor kinase, a phenylalanine in the Raf family, and valine in the JNK family. The p38 family is somewhat unique in that this residue is an alanine (Ala157), with ATP being supported by a leucine residue located on the activation loop. This creates an open channel one could exploit for selectivity. The substituent at the 2-postion of quinazoline inhibitors such as **1** is incapable of accessing this space. Replacement with a phthalazine-based inhibitor with a substituent at the 1-position would enable a close contact to Ala157 and lead to increased selectivity. Additionally p38α contains a glycine residue adjacent to the linker strand Met109. This residue is present in only 40 kinases and is referenced for its ability to "flip", orienting the NH into the ATP binding pocket, where in other proteins this would be a carbonyl.[7] Unlike the quinazoline ring system, the phthalazine scaffold contains a nitrogen positioned so it could accept a hydrogen bond from the N−H of Gly110 and would facilitate engagement of the flipped glycine to potentially further improve selectivity.

Chemistry

Scheme 1 outlines the synthetic routes used to access the 1-aminophthalazines (**7**−**10**) starting from 6-bromo-1-chlorophthalazine (**2**).[8] Nucleophilic displacement of the chloride with an appropriate amine followed by a Suzuki coupling with boronic ester **6**[9] provided aminophthalazines **7**−**9**. In situ generation of the boronic ester of **4** followed by Suzuki coupling with **11** afforded **10**.

Phthalazine ethers were prepared in an analogous manner (Scheme 2). Reaction of the sodium salt of *i*-PrOH or 1,1,1-trifluoro-2-propanol with **2** afforded **12** and **13**. The cyclopropylamide tolyl fragment was appended as previously described to furnish phthalazine ethers **15**, **16**, and **17**. Separation of the enantiomers, **16** and **17**, was accomplished using supercritical fluid chromatography on chiral stationary phase (see Experimental Section). The 1-aryl substituted phthalazines (**18** and **19**) were accessed from **2** by sequential cross-coupling reactions.

Isoquinoline **20** was prepared from 4,7-dibromoisoquinoline[10] by a selective Suzuki coupling of **6** followed by a palladium mediated coupling of isopropanol (Scheme 3).

Results and Discussion

Replacement of the quinazoline ring with a phthalazine (**1** versus **7**) resulted in similar inhibitory activity for p38α ($IC_{50} \approx 1$ nM) but a large increase in selectivity against other kinases (Table 1). The lower selectivity of **8** against cKit (440-fold) could be increased to >1500-fold by introduction of a methyl substituent (**9**). This effect was also seen in the 1-aryl series, where **19** exhibited >2500-fold selectivity over cKit in contrast to the unsubstituted congener **18**. This increase of selectivity was attributed to the methyl group being in proximity to Ala157 in p38α versus clashing with the more bulky Leu799 in cKit. Removal of the methyl group on the toluamide ring (**10**) had a negative impact on activity on all kinases. This is likely due to the loss of an important hydrophobic interaction with the gatekeeper pocket and the ability to more easily adopt a coplanar relationship between the two rings. The ethers **15** and **16** showed similar selectivity; expansion of the counter screening panel on **16** revealed modest activities against Lyn (IC_{50}= 954 nM) and PDGFR (IC_{50}= 88 nM). The activity on the PDGF receptor kinase was unexpected, since this protein, analogous to cKit and Lyn, bears a leucine residue at the Ala157 position of p38α. We can offer no structural rationale for the ability of PDGF receptor kinase to bind compound **16**, save possibly an increased plasticity of this protein.

A cocrystal structure of **19** bound to p38α (Figure 3) was obtained; gratifyingly the phthalazine accepts hydrogen bonds from the linker Met109 and the now flipped Gly110. As a consequence of this rotation, the two N-terminal residues are drawn in to engage the tolyl ring through van der Waals

Scheme 2. Synthesis of 1-Ether and Arylphthalazines (**15**−**19**)[a]

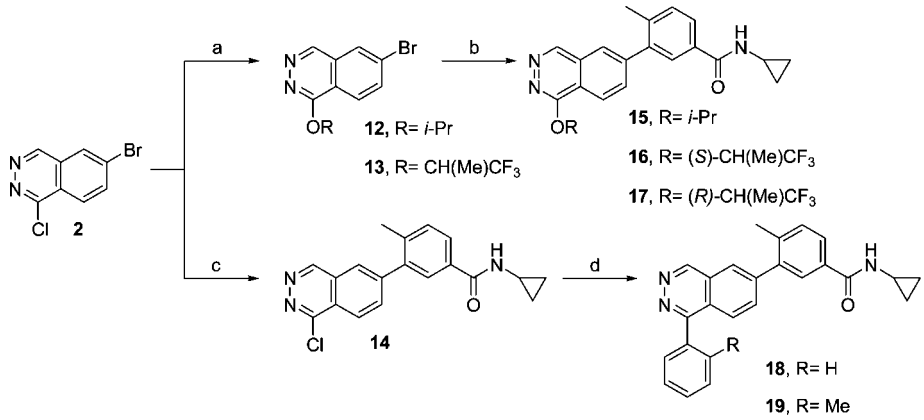

[a] Reagents: (a) NaH, ROH; (b) **6**, $Pd(PPh_3)_4$, 2 M aqueous Na_2CO_3, DME/EtOH, 90 °C; for **16** and **17**: Pd $(PPh_3)_4$, 2 M aqueous Na_2CO_3, dioxane, 125 °C; (c) **6**, $Pd(PPh_3)_4$, 2 M aqueous K_2CO_3, DME/EtOH, 70 °C; (d) $ArB(OH)_2$, $Pd(PPh_3)_4$, 2 M aqueous K_2CO_3, DME/EtOH, 95 °C.

Scheme 3. Synthesis of Isoquinoline **20**[a]

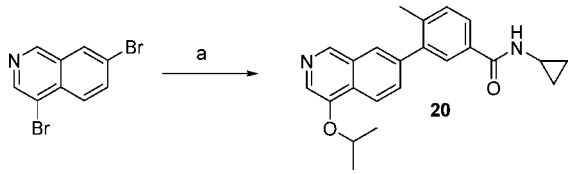

[a] Reagents: (a) (i) **6**, $Pd(PPh_3)_4$, 1 M aqueous Na_2CO_3, DME, reflux; (ii) *i*-PrOH, $Pd(OAc)_2$, 2-di-*tert*-butylphosphino-1,1′-naphthyl, Cs_2CO_3, toluene, 80 °C.

interactions. The methyl substituent forces the ring to adopt a perpendicular conformer and engages Ala157 on the floor of the ATP binding pocket. All other interactions are analogous to those observed in the cocrystal of **1** and p38α (Figure 2).

To interrogate further the contribution of the glycine flip to kinase selectivity, a matched pair of inhibitors that do not fully engage Ala157 was prepared and evaluated. Phthalazine **15**, which is capable of inducing a conformational change in p38α that would necessarily encounter a deleterious interaction with the carbonyl group of non-glycine-containing enzymes, was compared to isoquinoline **20**, which is incapable of inducing a conformational change but provides a C−H donor satisfying both a nonflipped glycine and a non-glycine-containing enzyme. We employed cKit as prototypical non-glycine-containing enzyme (Table 2). While inhibitory activity against p38α for **15** and **20** is equivalent, the selectivity against cKit was improved 10-fold for **15**.

The compounds were evaluated for their inhibitory effect on the production of TNFα in LPS-stimulated THP-1 cells and on the production of IL-8 in TNF-stimulated human whole blood. Phthalazine **7** was equipotent in the THP-1 cellular and 2-fold more potent in the whole blood assays when compared to quinazoline **1** (Table 3). Removal of the ethylene linker gave **8**, which displayed a 35-fold increase in efficacy in the cellular assay and a 5-fold increase in the whole blood assay versus **7**. The increased potency of **8** may be a result of the difference in cellular permeability between **7** and **8**. In the Caco-2 system, **7** exhibited lower permeability ($P_{app}(A>B) = 0.3 \times 10^{-6}$ cm/s, $P_{app}(B>A) = 31.0 \times 10^{-6}$ cm/s) compared to **8** ($P_{app}(A>B) = 10.5 \times 10^{-6}$ cm/s, $P_{app}(B>A) = 39.8 \times 10^{-6}$ cm/s). Compound **9** was equipotent to **8** in the cellular and whole blood assays. The isopropyl ether analogue **15** exhibited low single digit nanomolar activity in the cellular and whole blood assays. Replacement of one of the methyl groups for a trifluoromethyl group delivered the enantiomers **16** and **17**. The *S*-enantiomer (**16**) maintained low single digit nanomolar potency, while **17** displayed a 2-fold decrease in potency. Both **18** and **19** were very potent in the cellular ($IC_{50} \approx 1$ nM) and whole blood ($IC_{50} = 2-4$ nM) assays.

Pharmacokinetics. In Sprague−Dawley rats, compound **7** displayed low bioavailability (1%) and exposure (39 ng·h/mL), while **8** exhibited a moderate plasma clearance (1.7 (L/h)/kg). Studies in rat liver microsomes identified the morpholine ring as the major site of metabolism; incorporation of a methyl substituent on the morpholine (**9**) somewhat ameliorated this issue (CL= 0.8 (L/h)/kg). The phenyl series exemplified by compound **19** also displayed less favorable pharmacokinetics (CL = 1.7 (L/h)/kg, $t_{1/2} = 1.4$ h). Ether **16** demonstrated a lower plasma clearance (0.35 (L/h)/kg) and consequently a longer half-life (9.9 h) compared to its nonhalogenated congener **15** (CL = 0.85 (L/h)/kg, $t_{1/2} = 1.8$ h; Table 4).

In Vivo Studies. Compound **16** exhibited a dose-dependent inhibition of the production of TNFα in rats stimulated by an LPS challenge with an ED_{50} of <0.03 mg/kg (Figure 4). The mean terminal plasma concentration at the ED_{50} was <3 nM, which is consistent with its in vitro inhibitory effect in the presence of whole blood (TNFα /IL-8 $IC_{50} = 2.7$ nM, Table 3). The efficacy of **16** was also evaluated in a collagen induced arthritis (CIA) disease study in Lewis rats (Figure 5). Compound **16** demonstrated an ED_{50} of 0.04 mg/kg, and the AUC (0−24 h) was estimated to be 123 nM·h at the ED_{50}.

Conclusions

The cocrystal of quinazoline **1** with p38α provided insights to further exploit a number of features unique to this enzyme. A phthalazine-based series (**7**−**10**, **15**−**19**) was prepared and shown to be potent and selective inhibitors of p38α. The X-ray crystal structure of **19** bound to p38α illustrated that these compounds engage an uncommon floor residue, Ala157, and induce a conformational rotation of a glycine residue. Further investigation led to **16**, an agent with desirable pharmacokinetic properties. In vivo studies revealed **16** exhibited potent inhibition of TNF-α production (ED_{50} < 0.03 mg/kg) and low dose efficacy in the CIA model ($ED_{50} = 0.04$ mg/kg).

Experimental Section

Chemistry. All reactions were carried out under nitrogen or argon atmosphere unless otherwise noted. All solvents were purchased from Aldrich and used without further purification unless otherwise noted. Reactions performed under microwave irradiation

Table 1. Selectivity Profile of Quinazoline **1** and Phthalazines **7**−**10** and **15**−**19**[a]

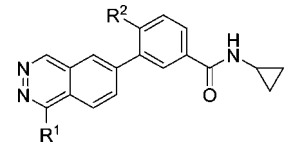

Compound	R^1	R^2	IC_{50} (nM) p38α	Kdr	Lck	cKit	JNK1	JNK2	JNK3
1	--	--	2.4±1.3	10.5*	122±20	162*	>10,000*	629*	788*
7	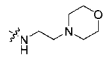	Me	1.9±1.0	5145	>10,000	1061	>10,000	>10,000	>10,000
8		Me	1.2±0.8	3042±480	3814±1360	529±75	>10,000	9685±1758	>10,000
9		Me	1.1±0.2	8553*	>10,000*	2007	>10,000*	4831*	>10,000
10		H	182	>10,000*	>10,000*	>8331	>10,000^	>10,000^	>10,000^
15		Me	0.6±0.4	1145*	3614±1957	421±32	>10,000*	5954*	>10,000*
16		Me	1.0±0.9	2680*	>5000^	1061±191	>10,000^	7772*	>10,000^
17		Me	0.8±0.4	505*	6048*	1174±361	>10,000^	4390±1232	9487±768
18		Me	2.0±1.7	6292*	1335*	149	>10,000	>10,000	>10,000
19		Me	0.8±0.6	>10,000*	>10,000*	2944*	>10,000*	5524*	6626*

[a] Standard deviations are given when $n \geq 3$. ∗ designates an average of two values. ∧ indicates a value for $n > 2$.

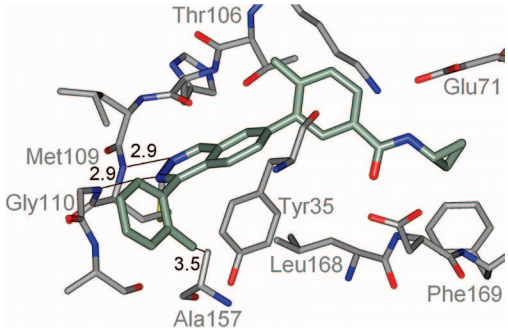

Figure 3. X-ray crystal structure of **19** bound to p38α.

were carried out on a Biotage Initiator Sixty Microwave Synthesizer. Medium pressure chromatography was performed using a Combi-Flash Companion (Teledyne ISCO) with RediSep normal-phase silica gel (35−60 μM) columns and UV detection at 254 nm. Preparative reverse-phase HPLC was performed on a Gilson 215 liquid handler equipped with a Phenomenex Synergi Max-RP column (150 × 21.2 mm, 4.0 μm) with UV detection at 254 nm, eluting with 10−100% CH_3CN in water with 0.1% TFA for 12 min at 20 mL/min. Final analytical LCMS methods were performed with an Aglient 1100 series instrument and UV detection at 254 nm, and a low resonance electrospray mode (ESI) with a binary solvent system of 0.1% TFA in water (system A) and 0.1% TFA in CH_3CN (system B). Method LCMS-1 uses a Zorbax SB-C18 column (3.0 mm × 50 mm, 3.5 μm), 40 °C column temperature, and 2.00 μL injection volume, eluting with the following gradients: 0.0−3.0 min, 10−95% B; 3.0−3.5 min, 95% B; 3.51 min, 10% B at 1.5 mL/min. Method LCMS-2 uses a YMC ODS-AM C-18 column (100 mm × 21 mm, 5 μm), 40 °C column temperature, 3 μL injection volume, eluting with the following gradients: 0.0−0.5 min, 10% B; 0.5−7.0 min, 10−100% B; 7.0−9.5 min, 100% B; 9.5−10.0 min, 100−10% B at 0.5 mL/min. Method LCMS-3 uses a Luna C18(2) column (100 mm × 4.6 mm, 5 μm), 40 °C column temperature, 3 μL injection volume, eluting with the following

Table 2. Inhibitory Activity of Phthalazine **15** and Isoquinoline **20** toward p38α and cKit[a]

Compound	IC_{50} (nM) p38α	cKit	Fold Selectivity
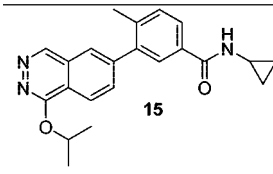 **15**	0.6±0.4	421±32	700
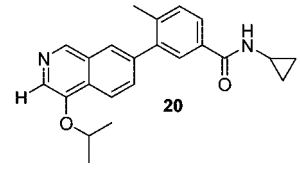 **20**	0.6*	41±19	68

[a] Standard deviations are given when $n \geq 3$. ∗ designates an average of two values.

Table 3. Cellular and Human Whole-Blood Activity of Quinazoline **1** and Phthalazines **7**−**9** and **15**−**19**

	IC_{50} (nM)	
compd	THP-1/TNFα	hWB TNFα/IL-8
1	24.7 ± 21.5	10.7 ± 4.8
7	24.9 ± 18.9	4.3 ± 0.6
8	0.7 ± 0.2	0.9 ± 0.3
9	1.1 ± 0.6	1.2 ± 1.0
15	0.4 ± 0.03	1.6 ± 0.9
16	0.4 ± 0.2	2.7 ± 1.1
17	0.9 ± 0.1	8.1 ± 2.7
18	0.8 ± 0.3	3.5 ± 0.4
19	0.4 ± 0.1	2.5 ± 0.8

Table 4. PK Profile in Sprague−Dawley Rats following Intravenous (iv) and Oral (po) Dose[a]

	iv (2.0 mg/kg in DMSO)			po (10 mg/kg)	
compd	CL ((L/h)/kg)	V_{dss} (L/kg)	$t_{1/2}$ (h)	$AUC_{(0-\infty)}$ (ng·h/mL)	*F* (%)
7	1.2	2.8	2.3	39[c]	1
8[b]	1.7	3.5	4.1	124[c]	22
9	0.8	1.2	1.3	7089[d]	57
19	1.7	1.8	1.4	2332[c]	40
15	0.8	2.1	1.8	10933[d]	92
16	0.35	4.7	9.9	21097[d]	72

[a] Values for are an average of three rats. [b] Dosed iv and po at 1 mg/kg. [c] Vehicle = 2% HPMC/1% Tween-80. [d] Vehicle = 1% Tween-80 in OraPlus, pH 2.2.

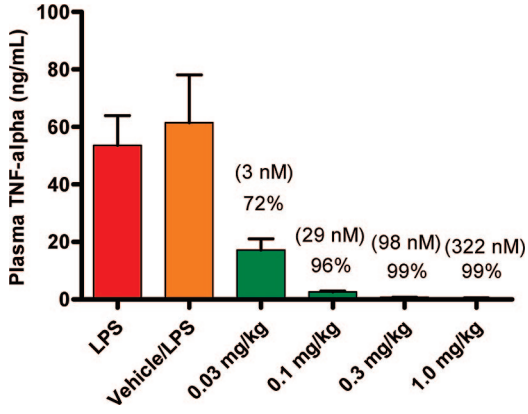

Figure 4. Effect of **16** on LPS-Induced TNFα in Lewis rats.

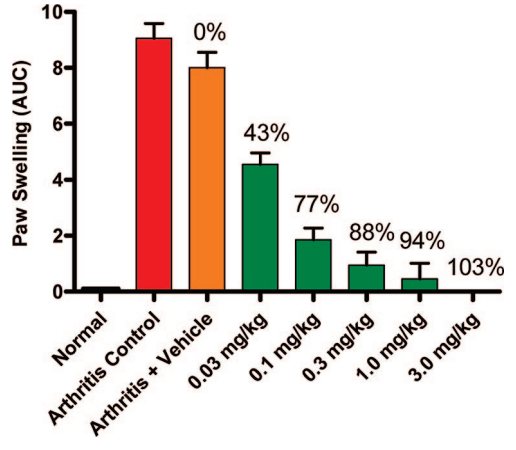

Figure 5. Efficacy of **16** in collagen-induced arthritis in Lewis rats.

gradients: 0.0−9.0 min, 5−95% B; 9.0−9.5 min, 95% B; 9.5−10.0 min, 5% B at 1.0 mL/min. Method LCMS-4 uses a Zorbax SB-C18 column (4.6 mm × 30 mm, 1.8 μm), 45 °C column temperature, 1 μL injection volume, eluting with the following gradients: 0.00−0.05 min, 0−20% B; 0.05−0.4 min, 20−80% B; 0.4−0.8 min, 80−100% B; 0.8−1.0 min, 100% B at 2.8 mL/min. Method LCMS-5 uses a Phenomenex Synergi MAX-RP column (2.0 mm × 50 mm, 4 μm), 40 °C column temperature, 3.00 μL injection volume, eluting with the following gradients: 0.0−0.2 min, 0−10% B; 0.2−3.0 min, 10−100% B; 3.0−4.5 min, 100% B; 4.5−5.0 min, 100−10% B at 0.8 mL/min. Preparative chiral supercritical fluid chromatography (SFC) was performed on a Berger Multigram II SFC with a Chiralpak AD-H column (21 mm × 250 mm, 5 μm) with liquid CO_2 (system A) and MeOH (system B): column temperature 40 °C, 60 mL/min flow rate, 100 bar outlet pressure, isocratic elution 65:35 (A/B). Analytical chiral SFC was performed on a Chiralpak AD-H (150 mm × 4.6 mm, 5 μm): column temperature 40 °C, 4.0 mL/min flow rate, 100 bar outlet pressure, isocratic elution 65:35 (A/B). ^{1}H NMR spectra were recorded on a Bruker AV-400 (400 MHz) or Bruker DPX-300 (300 MHz) spectrometer at ambient temperature. Elemental analyses were performed by Atlantic Microlab, Inc. Norcross, GA, and were within ±0.4% of the theoretical values.

***N*-Cyclopropyl-4-methyl-3-(2-((2-(4-morpholinyl)ethyl)amino)-6-quinazolinyl)benzamide (1).** A mixture of 6-bromo-*N*-(2-morpholinoethyl)quinazolin-2-amine[11] (200 mg, 0.68 mmol), **6** (225 mg, 0.75 mmol), $Pd(PPh_3)_4$ (78 mg, 0.068 mmol), and 2 M Na_2CO_3 (0.68 mL, 1.36 mmol) in 5 mL of 4/1 toluene/EtOH was heated at 80 °C for 3 h. After cooling, the reaction mixture was filtered through a 0.45 μm filter. Saturated $NaHCO_3$ (aq) was added, and the mixture was extracted with EtOAc (3×). The combined organic layers were dried over Na_2SO_4, filtered, and concentrated. The crude product was purified by silica gel chromatography (0−5% MeOH in CH_2Cl_2) to afford the title compound (170 mg, 58%) as an off-white solid. ^{1}H NMR ($CDCl_3$, 400 MHz): δ 8.99 (s, 1H), 7.66−7.59 (m, 5H), 7.34 (d, *J* = 8.53 Hz, 1H), 6.22 (s, 1H), 5.88 (s, 1H), 3.76−3.74 (m, 4H), 3.69−3.64 (m, 2H), 2.93−2.89 (m, 1H), 2.69−2.66 (m, 2H), 2.54 (br s, 4H), 2.32 (s, 3H), 0.90 (m, 2H), 0.64−0.60 (m, 2H). LCMS-1: *m*/*z* = 432.2 $[M + H]^+$, t_R= 1.62 min (100%). HRMS ($[M + H]^+$) calcd 432.239 40; found 432.234 27.

6-Bromo-*N*-(2-(4-morpholinyl)ethyl)-1-phthalazinamine (3). A mixture of **2**[8] (0.30 g, 1.23 mmol) and 4-(2-aminoethyl)morpholine (0.32 mL, 2.46 mmol) in 1 mL of *i*-PrOH was heated in a microwave at 180 °C for 5 min. The mixture was concentrated and purified by silica gel chromatography (5% MeOH in CH_2Cl_2) to furnish the title compound (320 mg, 77%) as a pale-yellow solid. ^{1}H NMR ($CDCl_3$, 400 MHz): δ 8.86 (s, 3 H), 7.97 (d, *J* = 1.96 Hz, 1 H), 7.89 (dd, *J* = 8.80, 1.96 Hz, 1 H), 7.67 (d, *J* = 8.61 Hz, 1 H), 3.77−3.75 (m, 6 H), 2.79−2.75 (m, 2 H), 2.59−2.46 (m, 4 H). LCMS-2: *m*/*z* = 337/339 $[M + H]^+$, t_R= 0.81 min (97.3%).

6-Bromo-1-(4-morpholinyl)phthalazine (4). A mixture of **2** (0.123 g, 0.5 mmol), morpholine (0.087 mL, 1.0 mmol), and K_2CO_3 (70.0 mg, 0.5 mmol) in 5 mL of CH_3CN was heated in microwave at 160 °C for 10 min. The mixture was concentrated and purified by silica gel chromatography (5% MeOH in CH_2Cl_2) to give the title compound (140 mg, 95%) as a pale-yellow solid. ^{1}H NMR ($CDCl_3$, 400 MHz): δ 9.12 (s, 1H), 8.06 (s, 1 H), 7.91 (d, *J* = 0.98 Hz, 2 H), 4.00−3.95 (m, 4H), 3.57−3.53 (m, 4 H). LCMS-3: *m*/*z* = 294/296 $[M + H]^+$, t_R= 4.37 min (98.5%).

6-Bromo-1-((3*S*)-3-methyl-4-(morpholinyl)phthalazine (5). A solution of (*S*)-3-methylmorpholine-PTSA salt (1.51 g, 5.5 mmol) in MeOH (11 mL) was prepared using a sonicator. The solution was treated with MP-carbonate (2.9 g), and the mixture was stirred at room temperature for 3 h. It was then filtered through a sintered glass frit, washed with $CHCl_3$, and concentrated. The residue was redissolved in CH_3CN (6.9 mL) and combined with **2** (340 mg, 1.4 mmol) and Cs_2CO_3 (1.8 g, 5.5 mmol). This reaction mixture was heated in the microwave for 30 min at 200 °C and then diluted with 20 mL of EtOAc and washed three times with 20 mL of saturated $NaHCO_3$ (aqueous). The organic layer was dried over Na_2SO_4, filtered, and concentrated. The crude material was purified by silica gel chromatography (0−6% (2 M ammonia in MeOH) in CH_2Cl_2) to afford the title compound (340 mg, 80% yield) as a white solid. ^{1}H NMR ($CDCl_3$, 400 MHz): δ 9.14 (s, 1 H), 8.06 (d,

J = 1.76 Hz, 1 H), 8.00−7.95 (m, 1 H), 7.94−7.88 (m, 1 H), 4.06−4.00 (m, 2 H), 4.00−3.88 (m, 2 H), 3.69−3.58 (m, 2 H), 3.41−3.33 (m, 1 H), 1.20 (d, J = 6.26 Hz, 3 H). LCMS-2: m/z = 308, 310 $[M + H]^+$, t_R= 3.86 min (97.2%).

***N*-Cyclopropyl-4-methyl-3-(1-((2-(4-morpholino)ethyl)amino)-6-phthalazinyl)benzamide (7).** A mixture of **3** (220 mg, 0.65 mmol) and **6** (197 mg, 0.65 mmol) in 20 mL of DME/EtOH (4/1) was treated with 2 M K_2CO_3 (aqueous, 1 mL, 2 mmol) and $Pd(PPh_3)_4$ (38 mg, 0.033 mmol). The mixture was stirred at 90 °C for 1 h and then cooled to room temperature and diluted with 100 mL of CH_2Cl_2. The organic layer was washed with 20 mL of brine, dried over anhydrous Na_2SO_4, filtered, and concentrated. The crude material was purified by silica gel chromatography (1−10% MeOH in CH_2Cl_2) to furnish the title compound (220 mg, 71%) as a pale-yellow solid. ^{1}H NMR ($CDCl_3$, 400 MHz): δ 8.92 (s, 1 H), 7.89−7.84 (m, 1 H), 7.77−7.72 (m, 1 H), 7.74−7.66 (m, 3 H), 7.39−7.37 (m, 1 H), 6.51−6.41 (m, 1 H), 3.83−3.75 (m, 6 H), 2.99−2.88 (m, 1 H), 2.82−2.74 (m, 2 H), 2.58 (d, J = 3.72 Hz, 4 H), 2.31 (s, 3 H), 0.93−0.83 (m, 2 H), 0.69−0.59 (m, 2 H). LCMS-1: m/z = 432 $[M + H]^+$, t_R= 1.18 min (98.3%). HRMS ($[M + H]^+$) calcd 432.239 40; found 432.235 68.

***N*-Cyclopropyl-4-methyl-3-(1-(4-morpholino)-6-phthalazinyl)-benzamide (8). 8** was prepared from **4** (130 mg, 0.44 mmol) in a manner analogous to example **7**. The crude material was purified by silica gel chromatography (1−10% MeOH in CH_2Cl_2) to give the title compound (150 mg, 90%) as a pale-yellow solid. ^{1}H NMR ($CDCl_3$, 400 MHz): δ 9.21 (s, 1 H), 8.10 (d, J = 8.41 Hz, 1 H), 7.83 (s, 1 H), 7.79 (dd, J = 8.51, 1.47 Hz, 1 H), 7.70−7.67 (m, 2 H), 7.39 (d, J = 8.02 Hz, 1 H), 4.04−3.99 (m, 4 H), 3.63−3.58 (m, 4 H), 2.94−2.90 (m, 1H), 2.32 (s, 3 H), 0.91−0.86 (m, 2 H), 0.65−0.61 (m, 2 H). MS m/z = 389 $[M + H]^+$. Anal. ($C_{23}H_{24}N_4O_2$) C, H, N. HRMS ($[M + H]^+$) calcd 389.239 40; found 389.188 84.

***N*-Cyclopropyl-4-methyl-3-(1-((3*S*)-3-methyl-4-morpholinyl)-6-phthalazinyl)benzamide (9).** A mixture of **6** (317 mg, 1.05 mmol), **5** (270 g, 876 μmol), $Pd(PPh_3)_4$ (101 mg, 88 μmol), and 1.5 M K_2CO_3 (aqueous, 1.75 mL, 2.63 mmol) in EtOH (9 mL) was heated at 80 °C for 1 h. The reaction mixture was diluted with 100 mL of EtOAc and washed three times with 50 mL of saturated $NaHCO_3$ (aqueous). The organic layer was dried over Na_2SO_4 and concentrated. The crude product was purified by reverse-phase preparative HPLC, and the collected fractions were basified with saturated $NaHCO_3$ (aqueous). The aqueous phase was extracted with $CHCl_3$, and the organic layer was dried over anhydrous Na_2SO_4, filtered, and concentrated to give the title compound (130 mg, 37% yield) as a white solid. ^{1}H NMR ($CDCl_3$, 400 MHz): δ 8.12 (d, J = 8.41 Hz, 1 H), 7.82−7.69 (m, 4 H), 7.37 (d, J = 7.63 Hz, 1 H), 6.85 (s, 1 H), 4.13−3.85 (m, 4 H), 3.73−3.60 (m, 2 H), 3.40−3.27 (m, 1 H), 3.01−2.87 (m, 1 H), 2.31 (s, 3 H), 1.20 (d, J = 6.46 Hz, 3 H), 0.90−0.78 (m, 2 H), 0.69−0.60 (m, 2 H). LCMS-3: m/z = 403 $[M + H]^+$, t_R= 5.23 min (100%). HRMS ($[M + H]^+$) calcd 403.212 85; found 403.206 37.

***N*-Cyclopropyl-3-iodobenzamide (11).** 3-Iodobenzoic acid (4.79 g, 19.3 mmol) was suspended in $SOCl_2$ (19 mL) and stirred for 1 h at 70 °C. The reaction mixture was concentrated and azeotropically dried with toluene. The residue was dissolved in dioxane (19 mL), and *N,N*-diisopropylethylamine (13.5 mL, 77.3 mmol) and cyclopropylamine (6.77 mL, 96.6 mmol) were added and stirred for 16 h at room temperature. The reaction mixture was diluted with 75 mL of EtOAc, and the organic layer was partitioned with saturated $NaHCO_3$ (aqueous), washed twice with 50 mL of 3 N HCl (aqueous), dried over Na_2SO_4, filtered, and concentrated to give the title compound (2.31 g, 42% yield) as an off-white solid. ^{1}H NMR ($CDCl_3$, 400 MHz): δ 7.77 (d, J = 8.41 Hz, 2 H), 7.46 (d, J = 8.41 Hz, 2 H), 6.22 (s, 1 H), 2.80−2.98 (m, 1 H), 0.77−0.99 (m, 2 H), 0.55−0.69 (m, 2 H). LCMS-1: m/z = 288 $[M + H]^+$, t_R= 1.77 min (99.4%).

***N*-Cyclopropyl-3-(1-(4-morpholinyl)-6-phthalazinyl)benzamide (10).** A mixture of **4** (95 mg, 0.32 mmol), 1,1′-bis(diphenylphosphino)ferrocenepalladium dichloride (24 mg, 0.032 mmol), KOAc (95 mg, 0.97 mmol), and bis(pinacolato)diboron (90 mg, 0.36 mmol) in 1,4-dioxane (3 mL) was heated at 80 °C for 2.5 h. This reaction mixture was added to a mixture of **11** (111 mg, 388 μmol) and $Pd(PPh_3)_4$ (37 mg, 32 μmol) in EtOH (3.25 mL) and 1.5 M K_2CO_3 (aqueous, 0.86 mL, 1.29 mmol) and stirred for 2 h at 80 °C. The reaction mixture was diluted with 75 mL of EtOAc and washed three times with 50 mL of saturated $NaHCO_3$. The organic layer was dried over Na_2SO_4, filtered, and concentrated. The crude material was purified by reverse-phase preparative HPLC. The collected fractions were basified with saturated $NaHCO_3$ (aqueous) and extracted with $CHCl_3$. The organic phase was dried over Na_2SO_4 and concentrated to give the title compound (22 mg, 18%) as a white solid. ^{1}H NMR ($CDCl_3$, 400 MHz): δ 9.25 (s, 1 H), 8.20−8.01 (m, 3 H), 7.90 (d, J = 6.06 Hz, 2 H), 7.76 (d, J = 7.63 Hz, 2 H), 6.31 (s, 1 H), 4.05−3.97 (m, 3 H), 3.65−3.55 (m, 3 H), 3.20−2.88 (m, 1 H), 0.98−0.86 (m, 1 H), 0.71−0.62 (m, 1 H). LCMS-1: m/z = 375 $[M + H]^+$, t_R = 1.25 min (99.4%). HRMS ($[M + H]^+$) calcd 375.181 55; found 375.177 43.

6-Bromo-1-(1-methylethoxy)phthalazine (12). Sodium hydride (60% in mineral oil, 493 mg, 12.32 mmol) was carefully added to a suspension of **2** (600 mg, 2.46 mmol) in 5 mL of *i*-PrOH over 5 min at room temperature. The mixture was stirred at room temperature for 1 h and then diluted with MeOH and adsorbed on to silica gel. The crude product was purified by silica gel chromatography (0−20% EtOAc in hexanes) to afford the title compound (525 mg, 80%) as a yellow solid. ^{1}H NMR (300 MHz, $CDCl_3$): δ 9.08 (s, 1 H), 8.10 (d, J = 8.67 Hz, 1 H), 8.03 (d, J = 1.70 Hz, 1 H), 7.92 (dd, J = 8.67, 1.88 Hz, 1 H), 5.76 (sept, J = 6.19 Hz, 1 H), 1.50 (d, J = 6.22 Hz, 6 H). LCMS-2: m/z = 267/269 $[M + H]^+$, t_R= 5.12 min (98.3%).

***N*-Cyclopropyl-4-methyl-3-(1-(1-methylethoxy)-6-phthalazinyl)benzamide (15).** A solution of **12** (250 mg, 0.94 mmol), **7** (352 mg, 1.17 mmol), $Pd(PPh_3)_4$ (54 mg, 0.047 mmol), and 2 M Na_2CO_3 (aqueous, 1.40 mL, 2.81 mmol) in 5 mL of DME/EtOH (4/1) was heated at 90 °C for 20 h. The cooled reaction was diluted with CH_2Cl_2 and washed with saturated aqueous $NaHCO_3$ solution, dried over anhydrous $MgSO_4$, filtered, and concentrated. The crude product was purified by silica gel chromatography (1−5% MeOH in CH_2Cl_2) to afford the title compound (240 mg, 71% yield) as an off-white amorphous solid. ^{1}H NMR ($CDCl_3$, 400 MHz): δ 9.12 (s, 1 H), 8.26 (d, J = 8.41 Hz, 1 H), 7.81−7.73 (m, 2 H), 7.73−7.66 (m, 2 H), 7.37 (d, J = 7.82 Hz, 1 H), 6.38 (br s, 1 H), 5.85−5.73 (m, 1 H), 2.97−2.88 (m, 1 H), 2.29 (s, 3 H), 1.52 (d, J = 6.06 Hz, 6 H), 0.88 (q, J = 6.52 Hz, 2 H), and 0.67−0.60 (m, 2 H). MS m/z = 362.2 $[M + H]^+$. Anal. ($C_{22}H_{23}N_3O_2$) C, H, N. HRMS ($[M + H]^+$) calcd 362.186 30; found 362.190 46.

6-Bromo-1-(2,2,2-trifluoro-1-methylethoxy)phthalazine (13). A solution of 1,1,1-trifluoropropan-2-ol (1.9 g, 17 mmol) in 10 mL of THF and 3 mL of DMF at 0 °C was treated with NaH (60% in mineral oil, 0.50 g, 12 mmol) and stirred for 10 min. Compound **2** (1.38 g, 5.7 mmol) was added as a solid in small portions. After the reaction mixture was stirred at room temperature for 1 h, it was poured into an ice-cold saturated NH_4Cl solution and extracted twice with EtOAc. The combined organic layers were dried over Na_2SO_4 and concentrated. The residue was purified by silica gel chromatography (20−70% EtOAc in hexanes) to give the title compound (1.57 g, 86% yield) as an off-white amorphous solid. ^{1}H NMR ($CDCl_3$, 300 MHz): δ 9.16 (s, 1 H), 8.10 (m, 2 H), 7.99 (m, 1 H), 6.16 (m, 1 H), 1.67 (d, J = 6.5 Hz, 3 H). LCMS-5: m/z = 321.0/323.0 $[M + H]^+$, t_R = 3.22 min (100%).

***N*-Cyclopropyl-4-methyl-3-(1-((*S*)-2,2,2-trifluoro-1-methylethoxy)-6-phthalazinyl)benzamide (16) and *N*-Cyclopropyl-4-methyl-3-(1-((*R*)-2,2,2-trifluoro-1-methylethoxy)-6-phthalazinyl)benzamide (17).** A mixture of **13** (3.0 g, 9.3 mmol), **6** (3.2 g, 11 mmol), $Pd(PPh_3)_4$ (0.54 g, 0.47 mmol) in 1,4-dioxane (15 mL), and 2 M Na_2CO_3 (aqueous, 15 mL, 30.0 mmol) was heated at 125 °C in a microwave for 30 min. The reaction mixture was diluted with 250 mL of EtOAc and washed with 10 mL of 1 N NaOH (aqueous) followed by brine. The organic layer was dried over $MgSO_4$, filtered, and concentrated. The crude material was purified by silica gel chromatography (45−85% EtOAc in hexanes) to give *N*-cyclopropyl-4-methyl-3-(1-(1,1,1-trifluoropropan-2-yloxy)phthalazin-6-yl)benzamide (3.34 g, 86% yield) as an off-white

amorphous solid. ^{1}H NMR ($CDCl_3$, 300 MHz): δ 9.24 (s, 1 H), 8.30 (d, J = 8.2 Hz, 1 H), 7.87 (s, 1 H), 7.85 (s, 1 H), 7.69 (s, 1 H), 7.67 (s, 1 H), 7.40 (d, J = 8.4 Hz, 1 H), 6.25 (br, 1 H), 6.20 (m, 1 H), 2.92 (m, 1 H), 2.31 (s, 3 H), 1.69 (d, J = 6.5 Hz, 3 H), 0.87 (m, 2 H), 0.62 (m, 2 H). LCMS-5: m/z = 416.1 $[M + H]^+$, t_R = 3.08 min (100%).

The racemic material was dissolved in DME and subjected to preparative chiral SFC to provide 1.46 g of *N*-cyclopropyl-4-methyl-3-(1-((*R*)-1,1,1-trifluoropropan-2-yloxy)phthalazin-6-yl)benzamide (**17**) as a white solid. Analytical chiral SFC: t_R = 1.51 min. Anal. ($C_{22}H_{20}F_3N_3O_2$) C, H, N. HRMS ($[M + H]^+$) calcd 416.158 04; found 41.161 12. Also obtained was 1.50 g of *N*-cyclopropyl-4-methyl-3-(1-((*S*)-1,1,1-trifluoropropan-2-yloxy)phthalazin-6-yl)benzamide (**16**) as an off-white solid. Analytical chiral SFC: t_R = 2.45 min. Anal. ($C_{22}H_{20}F_3N_3O_2$) C, H, N. HRMS ($[M + H]^+$) calcd 416.158 04; found 416.150 93.

3-(1-Chloro-6-phthalazinyl)-*N*-cyclopropyl-4-methylbenzamide (14). A mixture of **2** (500 mg, 2.05 mmol), **6** (617 mg, 2.05 mmol), $Pd(PPh_3)_4$ (118 mg, 0.10 mmol), and 2 M K_2CO_3 (aqueous, 3.07 mL, 6.15 mmol) in 16 mL of DME/EtOH (4/1) was stirred at 70 °C for 1 h and then concentrated. The crude product was purified by silica gel chromatography (5% (2 M ammonia in MeOH) in CH_2Cl_2) to afford the title compound (650 mg, 94%) as a yellow solid. ^{1}H NMR ($CDCl_3$, 400 MHz): δ 9.46 (s, 1 H), 8.36 (d, J = 8.41 Hz, 1 H), 7.98 (dd, J = 8.41, 1.56 Hz, 2.30 (s, 3H), 0.91−0.86 (m, 2 H), 0.64−0.61 (m, 2 H). LCMS-5: m/z = 338$[M + H]^+$, t_R = 2.91 min (95.8%).

***N*-Cyclopropyl-4-methyl-3-(1-phenyl-6-phthalazinyl)benzamide (18).** A mixture of **14** (98 mg, 0.29 mmol), phenylboronic acid (35 mg, 0.29 mmol), and $Pd(PPh_3)_4$ (17 mg, 0.015 mmol) in 2 mL of DME/EtOH (4/1) was treated with 2 M K_2CO_3 (aqueous, 0.44 mL, 0.87 mmol) and then stirred at 95 °C for 30 min. The mixture was cooled down to room temperature and concentrated. The crude product was purified by silica gel chromatography (2−6% (2 M ammonia in MeOH) in CH_2Cl_2) to give the title compound (60 mg, 55%) as a pale-yellow solid. ^{1}H NMR ($CDCl_3$, 400 MHz): δ 9.45 (s, 1H), 8.06 (d, J = 8.53 Hz, 1H), 7.86 (s, 1H), 7.79−7.69 (m, 3H), 7.67−7.61 (m, 2H), 7.57−7.49 (m, 3H), 7.32 (d, J = 8.03 Hz, 1H), 6.33 (2, 1H), 2.89−2.79 (m, 1H), 2.26 (s, 3H), 0.85−0.75 (m, 2H), 0.59−0.52 (m, 2H). LCMS-1: m/z = 380.2 $[M + H]^+$, t_R= 1.65 (98.8%). HRMS ($[M + H]^+$) calcd 380.175 74; found 380.169 05.

***N*-Cyclopropyl-4-methyl-3-(1-(2-methylphenyl)-6-phthalazinyl)benzamide (19). 19** was prepared from **14** (130 mg, 0.44 mmol) and *o*-tolylboronic acid (64 mg, 0.47 mmol) in a manner analogous to example **18**. The crude material was purified by silica gel chromatography (2−6% (2 M ammonia in MeOH) in CH_2Cl_2) to give the title compound (130 mg, 70%) as a pale-yellow solid. ^{1}H NMR ($CDCl_3$, 400 MHz): δ 9.57 (s, 1 H), 7.95 (s, 1 H), 7.80−7.76 (m, 1 H), 7.72−7.68 (m, 3 H), 7.46−7.44 (m, 1 H), 7.42−7.36 (m, 4 H), 6.35 (s, 1 H), 2.94−2.90 (m, 1 H), 2.33 (s, 3 H), 2.16 (s, 3 H), 0.88−0.85 (m, 2 H), 0.64−0.60 (m, 2 H). LCMS-1: m/z = 394 $[M + H]^+$, t_R= 1.77 min (99.3%). HRMS ($[M + H]^+$) calcd 394.191 39; found 394.191 62.

***N*-Cyclopropyl-4-methyl-3-(4-(1-methylethoxy)-7-isoquinolinyl)benzamide (20).** A solution of 4,7-dibromoisoquinoline[10] (322 mg, 1.12 mmol), **6** (338 mg, 1.12 mmol), $Pd(PPh_3)_4$ (65 mg, 0.056 mmol), and 1 M sodium carbonate (aqueous, 2.24 mL, 2.24 mmol) in 7 mL of DME was heated to reflux and stirred for 16 h. After the mixture was cooled to room temperature, water was added and the mixture was extracted with EtOAc (3×). The combined organic layers were dried over anhydrous Na_2SO_4, filtered, and concentrated. The crude material was purified by silica gel chromatography (1−4% MeOH in CH_2Cl_2) to afford 3-(1-bromo-6-phthalazinyl)-*N*-cyclopropyl-4-methylbenzamide (114 mg, 0.30 mmol).

A solution of 3-(1-bromo-6-phthalazinyl)-*N*-cyclopropyl-4-methylbenzamide (220 mg, 0.58 mmol), *i*-PrOH (0.22 mL, 2.90 mmol), Cs_2CO_3 (560 mg, 1.70 mmol), $Pd(OAc)_2$ (16 mg, 0.069 mmol), and 2-di-*tert*-butylphosphino-1,1′-naphthyl (34 mg, 0.087 mmol) in 3 mL of toluene was stirred at 80 °C for 20 h. After cooling to room temperature, the mixture was diluted with CH_2Cl_2 and washed with water. The layers were separated, and the aqueous layer was extracted with CH_2Cl_2 (2×). The combined organic layers were dried over anhydrous Na_2SO_4, filtered, and concentrated. The crude material was purified by silica gel chromatography (1/1 to 6/1 EtOAc/hexane) to afford the title compound (50 mg, 0.14 mmol) as an off-white amorphous solid. ^{1}H NMR ($CDCl_3$, 400 MHz): δ 8.82 (s, 1 H), 8.24 (d, J = 9.04 Hz, 1 H), 8.09 (s, 1 H), 7.74−7.66 (m, 2H), 7.34 (d, J = 8.03 Hz, 1H), 6.68 (br s, 1H), 4.86−4.80 (m, 1H), 2.94−2.89 (m, 1H), 1.49 (d, J = 6.02 Hz, 6H), 0.87 (m, 2H), 0.82 (m, 2H). LCMS-5: m/z = 361$[M + H]^+$, t_R= 2.71 min (100%). HRMS ($[M + H]^+$) calcd 361.183 78; found 361.191 74.

p38 Kinase Reaction. The p38α kinase reaction was carried out in a polypropylene 96-well black round-bottom assay plate in a total volume of 30 μL of kinase reaction buffer (50 mM Tris, pH 7.5, 5 mM $MgCl_2$, 0.1 mg/mL BSA, 100 μM Na_3VO_4, and 0.5 mM DTT). Recombinant activated human p38 enzyme (1 nM) was mixed with 50 μM ATP and 100 nM GST-ATF2-Avitag, in the presence or absence of inhibitor. The mixture was allowed to incubate for 1 h at room temperature. The kinase reaction was terminated, and phospho-ATF2 was revealed by addition of 30 μL of HTRF detection buffer (100 mM HEPES, pH 7.5, 100 mM NaCl, 0.1% BSA, 0.05% Tween-20, and 10 mM EDTA) supplemented with 0.1 nM Eu-anti-pTP and 4 nM SA-APC. After a 1 h incubation at room temperature, the assay plate was read in a Discovery Plate Reader (Perkin-Elmer). The wells were excited with coherent 320 nm light, and the ratio of delayed (50 ms after excitation) emissions at 620 nm (native europium fluorescence) and 665 nm (europium fluorescence transferred to allophycocyanin, an index of substrate phosphorylation) was determined (Park, Y.-W.; Cummings, R. T.; Wu, L.; Zheng, S.; Cameron, P. M.; Woods, A.; Zaller, D. M.; Marcy, A. I.; Hermes, J. D. Homogeneous Proximity Tyrosine Kinase Assays: Scintillation Proximity Assay versus Homogeneous Time-Resolved Fluorescence. *Anal. Biochem*. **1999**, *269*, 94−104).

LPS-Induced TNF-α Production in THP-1 Cells. THP-1 cells were resuspended in fresh THP-1 media (RPMI 1640, 10% heat-inactivated FBS, 1× PGS, 1× NEAA, plus 30 μM βME) at a concentration of 1.5×10^6 cells/mL. An amount of 100 μL of cells per well was plated in a flat-bottom polystyrene 96-well tissue culture plate. Then 2 μg/mL of bacterial LPS (Sigma) was prepared in THP-1 media and transferred to the first 11 columns of a 96-well polypropylene plate. Column 12 contained only THP-1 media for the LO control. Compounds were dissolved in 100% DMSO and serially diluted 3-fold in a polypropylene 96-well microtiter plate (drug plate). Columns 6 and 12 were reserved as controls (HI controls and LO controls, respectively) and contained only DMSO. One microliter of inhibitor compound from the drug plate followed by 10 μL of LPS was transferred to the cell plate. The treated cells were induced to synthesize and secrete TNFα in a 37 °C humidified incubator with 5% CO_2 for 3 h. TNFα production was determined by transferring 50 μL of conditioned media to a 96-well small spot TNFα plate (MSD, Meso Scale Discovery) containing 100 μL of 2× Read buffer P supplemented with an anti-TNFα polyclonal Ab labeled with ruthenium (MSD-Sulfo-TAG-NHS ester). After an overnight incubation at room temperature with shaking, the reaction was read on the Sector Imager 6000 (MSD). A low voltage was applied to the ruthenylated TNFα immune complexes, which in the presence of TPA (the active component in the ECL reaction buffer, Read buffer P) resulted in a cyclical redox reaction generating light at 620 nm. The amount of secreted TNFα in the presence of compound compared with that in the presence of DMSO vehicle alone (HI control) was calculated using the following formula: % control (POC) = (compd − average LO)/(average HI − average LO) × 100.

TNFα Induced IL-8 Production in Human Whole Blood. Whole blood was drawn from healthy, nonmedicated volunteers into sodium heparin tubes. An amount of 100 μL of blood was then plated into 96-well tissue culture plates (BD). Ten point compound titrations were added to blood and incubated for 1 h at 37 °C, 5% CO_2. TNFα (Amgen) with a final concentration of 1 nM was then added to blood and incubated overnight (16−18 h) at 37 °C, 5% CO_2. Plasma was harvested, and cytokines were

measured by MSD (Meso Scale Discovery) ECL based antibody sandwich assay. All reagents were prepared in RPMI 1640, 10% v/v human serum AB (Gemini Bio-Products), 1× Pen/Strep/Glu. Final concentration of human whole blood was 50%. Data were analyzed using XLfit/Activity Base software package (IDBS).

Pharmacokinetic Studies. Male Sprague−Dawley rats were administered the compound intravenously as a solution in DMSO (1 or 2 mg/kg dose) or orally as a suspension in 2% hydroxypropylmethylcellulose with 1% Tween-80 or in 1% Tween-80 in OraPlus, pH 2.2 (1 or 10 mg/kg dose). Samples were taken at various times after dosing and analyzed for parent compound by LCMS.

Caco-2 Cell Permeability Studies. Human colon carcinoma cell line (Caco-2) was obtained from the American Type Culture Collection (ATCC, Manassas, VA). Cells were cultured in Dulbecco's modified Eagle medium (DMEM) (Invitrogen Corp., Carlsbad, CA) supplemented with a final concentration of 1% MEM nonessential amino acids, 1 mM L-glucose, 2% penicillin−streptomycin−glutamine, and 10% fetal bovine serum (Invitrogen Corp., Carlsbad, CA). Supplemented medium was filtered through a 0.2 μm filter prior to use. Cells were seeded at 1.4×10^5 cells/cm^2 (passages 36−44, day 0) onto 24-well BIOCOAT HTS Fibrillar Collagen MultiwellTM insert plates (BD Biosciences, Billerica, MA) and were cultured for 20 days in a CO_2 (5%) incubator maintained at 37 °C (model BBD 6220, Kendro Laboratory Products, Newtown, CT). Cell culture media were replaced every 2−3 days throughout the course of the culture. Prior to the transport experiment, culture medium was aspirated from both apical and basolateral wells and Caco-2 cells were rinsed twice with warmed (37 °C) Hank's balanced salt solution supplemented with 10 mM Hepes at pH 7.4 (HHBSS, Invitrogen, Grand Island, NY). HHBSS was removed from wells prior to dosing with test drugs at 10 μM in HHBSS in either apical or basolateral chambers. Receiver chambers were supplemented with 2% bovine serum albumin (BSA) in order to ensure the optimal recovery of transported agents. All apical and basolateral chambers contained 250 and 900 μL of HHBSS, respectively, during all transport experiments. Transport studies were incubated for 1 h at 37 °C on a shaking platform. At the end of the incubation period, 150 μL samples were collected from receiver reservoirs and analyzed by LCMS/MS on an API4000 (Applied Biosystems, Foster City, CA) triple quadrupole mass spectrometer interfaced with turbo IonSpray operating in positive mode using Analyst 1.3.1 software. The apparent permeability coefficient (P_{app}) of all tested agents was estimated from the slope of a plot of cumulative amount of the agent versus time based on the following equation:

$$P_{app} = (dQ/dt)/(AC_0)$$

where dQ/dt is the penetration rate of the agent (ng/s), A is the surface area of the cell layer on the Transwell (0.33 cm^2), and C_0 is the initial concentration of the test compound (ng/mL).

Lipopolysaccharide (LPS)-Induced TNF Study. Lipopolysaccharide (Sigma Chemical Co.) was diluted in phosphate buffered saline (PBS, Life Technologies) to a concentration of 500 μg/mL. The vehicle or compound **16** as a solution in 15% hydoxypropyl-β-cyclodextrin, 1% hydroxymethylcellulose, 1% Pluronic F68 was administrated orally to female Lewis rats ($n = 6$) 1 h prior to injection with LPS (100 μg/rat, iv, tail vein). Blood was harvested 90 min following the administration of LPS. Serum TNFα levels were analyzed using rat TNFα CytoSet kit from Biosource International. Data points represent the mean ± STE.

Collagen Induced Arthritis Model. Arthritis was induced by intradermal injection of Porcine type II collagen emulsified 1:1 in incomplete Freunds adjuvant (IFA). Animals were assigned to treatment groups at disease onset (study day 0), which occurred 10−12 days following immunization. Compound **16** or vehicle (1% Tween-80 in Oraplus, pH 2.2) was administered orally once a day for 7 days. Dexamethasone was administered once daily, sc, for 7 days. Paw diameter was measured daily from day 0 through day 7. Area under the paw swelling curve (AUC) was calculated and used to determine percent inhibition of inflammation compared with vehicle controls. Data points represent the mean ± STE ($n = 8$ rats/group).

X-ray Crystallography. The protein construct expression and purification were based on the work described previously with some modification (Wilson, K. P.; Fitzgibbon, M. J.; Caron, P. R.; Griffith, J. P.; Chen, W.; McCaffrey, P. G.; Chambers, S. P.; Su, M. S. *J. Biol. Chem.* **1996**, *271*, 27696−27700). Briefly, full length p38α was expressed as a fusion protein with an amino terminal poly-histidine tag and a thrombin cleavage site. The protein was expressed in *E. coli*, and the cells were lysed by sonication. After centrifugation, the p38α protein was captured with Talon resin (Clontech). The resin was extensively washed, and thrombin was added to the slurry to cleave the poly-histidine tag. The protein was further purified on a HiTrap Blue column followed by a HiTrap Q column (GE HealthcareLife Sciences). For both resins the protein was eluted with a 0−1 M NaCl gradient in a 20 mM Tris-HCl, pH 7.5, 5 mM dithiothreitol, 10% glyerol buffer. The protein was dialized against the final storage buffer of 50 mM HEPES at pH 7.5, 100 mM NaCl, 10 mM dithiothreitol, and 5% glycerol.

For crystallization trials, the protein was concentrated to 15 mg/mL and a 10-fold molar excess of either compound **1** or **19** was added. A wide range of crystallization conditions were tested using the vapor diffusion method. Crystals of p38α with **1** were obtained with 1.6 M ammonium sulfate and 100 mM HEPES at pH 7.5 at room temperature. Crystals of p38α with **19** were obtained with 31% PEG 4000, 100 mM Na citrate, pH 5.6, 200 mM ammonium acetate, and 10 mM dithiothreitol at room temperature.

The structures were solved by molecular replacement using epmr, refined using CNX (Accelrys), and manual rebuilding was done using the graphics program Quanta (Accelrys). The structure of **1** and p38α was refined to 2.8 Å with an *R*-factor of 0.214 and free *R*-factor of 0.279. The structure of **19** and p38α was refined to 2.9 Å with an *R*-factor of 0.228 and free *R*-factor of 0.319.

Supporting Information Available: Table of elemental analysis results of compounds **8** and **15**−**17**, HPLC analyses of compounds **1**, **7**, **9**, **10**, and **18**−**20**, SFC analysis of **16** and **17,** and crystal X-ray structure data for **1** and **19**. This material is available free of charge via the Internet at http://pubs.acs.org.

References

(1) (a) Saxne, T.; Palladino, M. J.; Heinegard, D.; Talal, N.; Wollheim, F. Detection of Tumor Necrosis Factor α but Not Tumor Necrosis Factor β in Rheumatoid Arthritis Synovial Fluid and Serum. *Arthritis Rheum.* **1988**, *31*, 1041–1045. (b) Arend, W.; Dayer, J. Cytokines and Cytokine Inhibitors or Antagonists in Rheumatoid Arthritis. *Arthritis Rheum.* **1990**, *33*, 305–315. For a recent review, see the following. (c) Tracey, D.; Klareskog, L.; Sasso, E. H.; Salfeld, J. G.; Tak, P. P. *Pharmacol. Ther.* **2008**, *117*, 244–279.

(2) (a) Jarvis, B.; Faulds, D. Etanercept: A Review of Its Use in Rheumatoid Arthritis. *Drugs* **1999**, *57*, 945–966. (b) Garrison, L.; McDonnell, N. D. Etanercept: Therapeutic Use in Patients with Rheumatoid Arthritis. *Ann. Rheum. Dis* **1999**, *58* (Suppl. 1), 65–69. (c) Mease, P. J.; Goffe, B. S.; Metz, J.; VanderStoep, A.; Finck, B.; Burge, D. J. Etanercept in the Treatment of Psoritatic Arthritis and Psoriasis: A Randomized Trial. *Lancet* **2000**, *356*, 385–390. (d) Carteron, N. L. Cytokines in Rheumatoid Arthritis: Trial and Tribulations. *Mol. Med. Today* **2000**, *6*, 315–323. (e) Maini, R.; St. Clair, E. W.; Breedveld, F.; Furst, F.; Kalden, J.; Weisman, M.; Smolen, J.; Emery, P.; Harriman, G.; Feldmann, M.; Lipsky, P. Infliximab (Chimeric Anti-Tumor Necrosis Factor Alpha Monoclonal Antibody) versus Placebo in Rheumatoid Arthritis Patients Receiving Concomitant Methotrexate: A Randomized Phase III Trial. *Lancet* **1999**, *354*, 1932–1939. (f) Present, D. H.; Rutgeerts, P.; Targan, S.; Hanauer, S. B.; Mayer, L.; van Hogezand, R. A.; Podolsky, D. K.; Sands, B. E.; Braakman, T.; DeWoody, K. L.; Schaible, T. F.; van Deventer, S. J. Infliximab for the Treatment of Fistulas in Patients with Crohn'S Disease. *N. Engl. J. Med.* **1999**, *340*, 1398–1405. (g) Bang, L. M.; Keating, G. M. Adalimumab, a Review of Its Use in Rheumatoid Arthritis. *BioDrugs* **2004**, *18*, 121–139.

(3) (a) Palladino, M. A.; Bahjat, F. R.; Theodorakis, E. A.; Moldawer, L. L. Anti-TNF-α Therapies: The Next Generation. *Nat. Rev. Drug Discovery* **2003**, *2*, 736–746. (b) Bongartz, T.; Sutton, A. J.; Sweeting, M. J.; Buchan, I.; Matteson, E. L.; Montori, V. Anti-TNF Antibody Therapy in Rheumatoid Arthritis and the Risk of Serious Infections

and Malignacies Systematic Review and Meta-analysis of Rare Harmful Effects in Randomized Controlled Trials. *JAMA, J. Am. Med. Assoc.* **2006**, *295*, 2275–2285.

(4) (a) Laydon, J. T.; McDonnell, P. C.; Gallagher, T. F.; Kumar, S.; Green, D.; McNulty, D.; Blumenthal, M. J.; Heyes, J. R. A Protein Kinase Involved in the Regulation of Inflammatory Cytokine Biosynthesis. *Nature* **1994**, *372*, 739–746. (b) Saklatvala, J. The p38 MAP Kinase Pathway as a Therapeutic Target in Inflammatory Disease. *Curr. Opin. Pharmacol.* **2004**, *4*, 372–377. (c) Kumar, S.; Boehm, J.; Lee, J. C. p38 MAP Kinases: Key Signalling Molecules as Therapeutic targets for Inflammatory Diseases. *Nat. Rev. Drug Discovery* **2003**, *2*, 717–726.

(5) O'Keefe, S. J.; Mudgett, J. S.; Cupo, S.; Parsons, J. N.; Chartrain, N. A.; Fitzgerald, C.; Chen, S.-L.; Lowitz, K.; Rasa, C.; Visco, D.; Luell, S.; Carballo-Jane, E.; Owens, K.; Zaller, D. M. Chemical Genetics Define the Roles of p38α and p38β in Acute and Chronic Inflammation. *J. Biol. Chem.* **2007**, *282*, 34663–34671.

(6) (a) Peifer, C.; Wagner, G.; Laufer, S. New Approaches to the Treatment of Inflammatory Disorders Small Molecule Inhibitors of p38 MAP Kinase. *Curr. Top. Med. Chem.* **2006**, *6*, 113–149. (b) Hynes, J., Jr.; Leftheris, K. Small Molecule p38 Inhibitors: Novel Structural Features and Advances from 2002−2005. *Curr. Top. Med. Chem.* **2005**, *5*, 967–985. (c) Dominguez, C.; Tamayo, C.; Zhang, D. p38 Inhibitors: Beyond Pyridinylimidazoles. *Expert Opin. Ther. Pat.* **2005**, *15*, 801–816. (d) Goldstein, D. M.; Gabriel, T. Pathway to the Clinic: Inhibition of p38 MAP Kinase. A Review of Ten Chemotypes Selected for Development. *Curr. Top. Med. Chem.* **2005**, *5*, 1017–1029.

(7) (a) Fitzgerald, C. E.; Patel, S. B.; Becker, J. W.; Cameron, P. M.; Zaller, D.; Pikounis, V. B.; O'Keefe, S. J.; Scapin, G. Structural Basis for p38α MAP Kinase Quinazolinone and Pyridol-Pyrimidine Inhibitor Specificity. *Nat. Struct. Biol.* **2003**, *10*, 764–769. (b) Stelmach, J. E.; Liu, L.; Sangita, P. B.; Pivnichny, J. V.; Scapin, G.; Singh, S.; Hop, C. E. C. A.; Wang, Z.; Strauss, J. R.; Cameron, P. M.; Michols, E. A.; O'Keefe, S. J.; O'Neill, E. A.; Schmatz, D. M.; Schwartz, C. D.; Thompson, C. M.; Zaller, D. M.; Doherty, J. B. Design and Synthesis of Potent, Orally Bioavailable Dihydroquinazolinone Inhibitors of p38 MAP Kinase. *Bioorg. Med. Chem. Lett.* **2003**, *13*, 277–280. (c) Angell, R. M.; Bamborough, P; Cleasby, A.; Cockerill, S. G.; Jones, K. L.; Mooney, C. J.; Somers, D, O.; Walker, A. L. Biphenyl Amide p38 Kinase Inhibitors 1: Discover and Binding Mode. *Bioorg. Med. Chem. Lett.* **2008**, *18*, 318–323.

(8) (a) Bakthavatchatam, R.; Blum, C. A.; Brielmann, H. L.; Caldwell, T. M.; De Lombaert, S. Substituted Quinazolin-4-ylamine Analogues. WO 030662209 A2, 2003. For an alternative synthesis, see the following: (b) Zhang, X.; Nirschl, A. A.; Zou, Y.; Priestly, E. S. Phenylglycinamide and Pyridylglycinamide Derivatives Useful as Anticoagulants. WO 07002313 A2, 2007.

(9) Angell, R. M.; Baldwin, I. R.; Bamborough, P.; Deboeck, N. M.; Longstaff, T.; Swanson, S. Preparation of Fused Heteroaryls, in Particular Benzisoxazoles and Indazoles for Use as p38 Inhibitors in the Treatment of Rheumatoid Arthritis. WO 04010995 A1, 2004.

(10) Barber, C. G.; Fish, P. V.; Dickinson, R. P. Isoquinoline as Urokinase Inhibitors. WO 9920608 A1, 1999.

(11) DiMauro, E. F.; Newcomb, J.; Nunes, J. J.; Bemis, J. E.; Boucher, C.; Buchanan, J. L.; Buckner, W. H.; Cee, V. J.; Chai, L.; Deak, H. L.; Epstein, L. F.; Faust, T.; Gallant, P.; Geuns-Meyer, S. D.; Gore, A.; Gu, Y.; Henkle, B.; Hodous, B. L.; Hsieh, F.; Huang, X.; Kim, J. L.; Lee, J. H.; Martin, M. W.; Masse, C. E.; McGowan, D. C.; Metz, D.; Mohn, D.; Morgenstern, K. A.; Oliveria-dos-Santos, A.; Patel, V. F.; Powers, D.; Rose, P. E.; Schneider, S.; Tomlinson, S. A.; Tudor, Y.-Y.; Turci, S. M.; Welcher, A. A.; White, R. D.; Zhao, H.; Zhu, L.; Zhu, X. Discovery of Aminoquinazolines as Potent, Orally Bioavailable Inhibitors of Lck: Synthesis, SAR and in Vivo Anti-Inflammatory Activity. *J. Med. Chem.* **2006**, *49*, 5671–5686.

JM8005417